



REPAIRING OF CONTINUOUS ONE-WAY REINFORCED CONCRETE SLABS BY CFRP COMPOSITES

Saif M. Aljbory¹ and Hayder H. Kamonna²

¹ M. Sc. Student, Faculty Engineering, University of Kufa, Iraq,
Email: saifa.aljbory@student.uokufa.edu.iq

² Prof. Dr., Faculty of Engineering, University of Kufa, Iraq,
Email: hayder.kammona@uokufa.edu.iq

<https://doi.org/10.30572/2018/KJE/160119>

ABSTRACT

This paper presents an experimental investigation of the performance of two-span reinforced concrete slabs repaired by CFRP composites against flexural loads. Thirteen continuous reinforced concrete (RC) one-way-slabs were cast, with dimensions of 2400 mm length, 500 mm width, and 100 mm thick. The first specimen had no strengthening at all and was considered a reference slab (Control). The rest of the slabs were repaired using different configurations of external bonding CFRP sheets and NSM bars. Before the repairing process, the slabs were subjected to 40% and 65% of the control slab ultimate load. The test was done under two-line loads. Moreover, the effect of different lengths, spacing, repairing techniques, and damage ratios were studied in this work. The finding shows that the repairing methods were effective in improving the ultimate load capacity ranges between 42% to 70% and reducing the deflection by about 11% to 25%.

KEYWORDS

One-way slabs, CFRP, externally bonded, Load-deflection curves, Near-surface mounted, Crack pattern.



1. INTRODUCTION

The rehabilitation of RC buildings has become more and more important, especially in the last few years. Many concrete structures are nearing the end of their service life which leads to a major need for concrete maintenance. Moreover, the deterioration commonly found in many reinforced concrete structures is often the result of deflections and cracks. Several factors can affect these, including earthquakes, vibrations, corrosion of reinforced bars, overloading, and environmental changes (Fayyadh and Razak, 2012). Additionally, Strengthening and repairing structural constructions takes less time and money to maintain structural elements than reconstructing them. Although, knowing and understanding the causes of cracks and deflections is significant to maintaining the structure choosing the suitable technique is still the most important also in long-term performance (Benjeddou et al., 2007).

Generally, there are several methods for strengthening and repairing different structural RC elements. One of these methods is using polymer fibers like glass, carbon, and other similar fiber-reinforced polymers (FRP). These fibers can effectively repair and strengthen concrete elements due to their mechanical and physical characteristics (Mstthys and Tearwe, 2000). Among these fibers, using carbon fibers has become known as an effective solution for a wide range of engineering problems due to their high strength-weight Ratio, durability, and corrosion Resistance (Wong RS, 2001; Hosen et al., 2014; Thi et al., 2015; Frhaan et al., 2021). Moreover, these fibers can be in the form of laminates and attached to the RC member using the externally bonded technique which includes the bonding of one or multiple FRP laminates to the tension region (Teng et al., 2003) or it can be in the form of rods and installed into the concrete using the Near-surface mounted technique (NSM). This method involves installing FRP strips or bars inside grooves created in the concrete cover, and then filling these grooves with epoxy adhesive (De Lorenzis and Teng, 2007). The common issue that faced the EBR technique is the early debonding caused by excessive bond and tensile shear stresses developing in the concrete near the adhesive layer. Generally speaking, these high stresses cause the FRP to deboned from the concrete (Aram et al., 2008; Martinelli et al., 2014; Li et al., 2014).

Numerous studies, both theoretical and experimental, have been conducted to investigate the behavior of externally strengthened reinforced concrete (RC) members. According to a group of researchers, reinforcing existing RC structures with carbon fiber reinforced polymer (CFRP) can improve their strength without the need for rebuilding or replacement. However, other studies have indicated that it can be challenging to fully restore the strength of damaged reinforced concrete structures, even with improvements or repairs (Frhaan et al., 2021). Moreover, some researchers investigated the repairing of continuous RC members. (Hamed et

al. 2018) examined the effect of preloading on the flexural behavior of continuous RC beams. CFRP sheets were used to repair two beams in the sagging and hogging moment regions. Two damage ratios were used 100% and 90%. According to their test results the load capacity increased by 51.5% and 68.5% respectively. Meanwhile, at mid-span, the deflection decreased by 19% and 16% respectively.

Additionally, the effects of near-surface mounted (NSM) bars on the behavior of a continuous one-way slab under static loads was investigated by Kamonna and Abd Al-Sada (2021). A total of seven RC slabs were cast and tested. The samples were strengthened by NSM bars. The lengths of NSM bars, the spacing between bars, and using different materials were the parametric of the study. The results shows that the ultimate load was enhanced by 156.25% to 225%.

This study involved an experimental examination to study the behavior of Two-span continuous reinforced concrete (RC) slabs that were repaired by bonding CFRP sheets or NSM bars. The findings related to the crack patterns, maximum loads, load vs deflection curves, ductility, stiffness, toughness, and crack widths are examined and analyzed.

2. EXPERIMENTAL PROGRAM

In this research, thirteen continuous RC one-way slabs were prepared and tested. The Samples were designed to fail in flexure following ACI 318-19. The first specimen is the control slab, which was unbounded and loaded until failure in a single phase. The other six RC slabs were preloaded with 40% of the control slab ultimate load and repaired using different configurations of external bonding CFRP sheets and NSM bars. The rest of the slabs were subjected to a preloading ratio of about 65% and then repaired in the same way. The first ratio 40% indicates the slab is cracked and the second preloaded ratio, which was 65%, indicates that the building is about to reach the service stage, which is an essential phase in building construction. The effect of different lengths, spacing, damage ratios, and the effects of adopting NSM and EB CFRP techniques were examined in this study.

2.1. Details of test slabs

All slab consists of two equal spans with dimensions of 2200 mm in length, 500 mm in width, and 100 mm in height where the effective spans were 1100 mm. Three $\phi 10$ steel bars were placed at 200 mm c/c in both positive and negative moment regions and served as the main longitudinal reinforcement for each slab. In addition, the top and bottom secondary reinforcements were made of $\phi 10$ steel bars placed at 380 mm spacing along the length of each slab as shown in Fig.1.

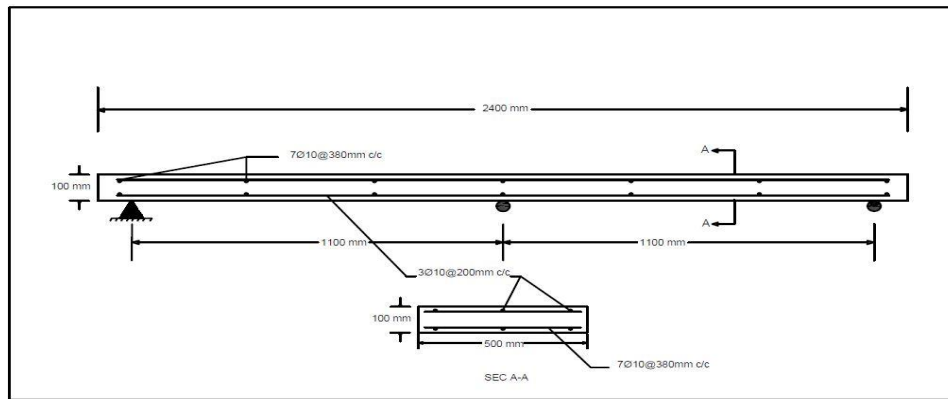


Fig.1. Details of typical slab

2.2. Materials

This section lists the characteristics of the cement, fine and coarse aggregate, admixture, carbon fiber reinforced polymer (CFRP), and epoxies that were utilized in the study.

2.2.1. Cement

The type of cement used in the concrete mix was **sulfate-resisting** Portland cement and was from AL-JESR /Lafarge Cement Karbala factory. The chemical and physical properties were agreed to the Iraqi Specifications (IQS) No.5/1984 ([Iraqi Specification, No.5, 1984](#)) requirements. The cubic compressive strength at 2 days and 28 days were equal to 22 and 44 MPa, respectively.

2.2.2. Fine aggregate

Natural fine aggregate was provided from the Sea of Najaf with 4.75 mm as the largest grain size. According to the sieve analysis, the grading was within Iraqi standard (IQS) No. 5/1984 ([Iraqi Specification, No. 5, 1984](#)) requirements.

2.2.3. Coarse aggregate

The type of coarse aggregate used in the concrete mix was local crushed gravel. The crushed gravel had a minimum size of 5 mm. The sieve analyses were all checked according to the Iraqi standard No.45/1984 ([Iraqi Specification, No.45, 1984](#)).

2.2.4. Superplasticizer (SP)

The superplasticizer that was used to create the concrete mixture has extremely low water-to-cement ratios while keeping workability levels normal known by its commercial name BETONAC® 200P-1. The SP complies with ASTM C494/C494M-15 ([ASTM C494/C494M-15, 2015](#)) Type G.

2.2.5. Steel bar reinforcement

The samples were reinforced with A1-mass bars. [Table 1](#) displays the results of the tensile test for three samples of steel bars compared to ASTM A615/615M-05a ([ASTM A615/615M-05a,2005](#)).

Table 1. Tensile strength test of the steel bar

No.	Diameter (mm)	Yielding stress fy MPa	Tensile stress fu MPa	Elongation (%)
Average	10	435	678	16.75
Limit ASTM A615	10	≥420	≥620	≥12

2.2.6. Carbon fiber reinforced polymer (CFRP) sheets

The Sika Wrap®-300C type carbon fiber fabric with fiber orientation 0° (unidirectional) has been selected as the material to be used for external bonding style to repair the continuous slabs.

Table 2 provides the characteristic of these sheets.

Table 2. Properties of CFRP sheets*

Type	Thickness, Mm	Weight, gm/m ²	Modulus of elasticity, MPa	Tensile strength, MPa	Elongation at break, %
Sika wrap 300-C	0.167	304± 10	230000	4000	1.7

*Supplied by the manufacturer

2.2.7. CFRP bars

The diameter of the CFRP bars utilized in the NSM strengthening was 6 mm. Table 3 describes the properties of carbon bars.

Table 3. Properties of carbon bars*

Properties	Value
Tensile strength	1800-2200 MPa
Elastic modulus	144-150 GPa
Elongation	1.3-1.5 %
Density	1.6-1.8 g/m ³

*Supplied by the manufacturer

2.2.8. Epoxy paste

Two types of epoxies were used in this work:

1. The brand name of the first epoxy paste that was used as an adhesive material to fix the CFRP sheets was Sikadur ®-330. However, it is made up of component A, a resin, and component B, a hardener. The mechanical characteristics of epoxy are shown in Table 4.

Table 4. Mechanical properties of epoxy paste Sikadur®-330*

Appearance	The ratio of mixing by (weight)	Density, kg/L	The strength of tensile, MPa	Elasticity modulus in tension, MPa	Break Elongation%
Component A: white	A: B	1.3	30	4500	0.9
Component B: grey	4:1				

*Supplied by the manufacturer

2. The second epoxy that was used to embed CFRP bars in the created grooves was Weber 412 cry plus. Also, it is made up of component A, a resin, and component B, a hardener. Moreover, the mechanical characteristics of this epoxy are shown in [Table 5](#).

Table 5. Properties of epoxy paste Weber 412 cry plus*

Appearance	The ratio of mixing by (weight)	Density, (g/cm ³)	Curing at 20°C
Component A: white	A: B	1.41	1 day
Component B: black	2:1		

*Supplied by the manufacturer

2.2.9. Concrete mixture

Ready-mix concrete was used to cast all slab specimens. The material quantities are listed in [Table 6](#). The results of compressive strength, splitting tensile strength, and modulus of rupture tests according to the BS1881-Part-116, ASTM C496 / C496M ([ASTM C496/C496M, 2011](#)), ASTM C78/C78M ([ASTM C78/C78M, 2015](#)) were 27 MPa, 2.16 MPa, and 5.21 MPa respectively.

Table 6. Materials quantities of concrete mixture

Materials	Quantity	Units	Mixing ratios%
Cement	400	Kg/m ³	1
Water	200	Kg/m ³	0.5
Sand	800	Kg/m ³	2
Gravel	1100	Kg/m ³	2.75
Superplasticizer	3	Liter/m ³	0.0075

2.2.10. Repairing Procedure

1. As seen in [Fig. 2](#), there are a few steps to follow when adhering the sheets to the slabs:

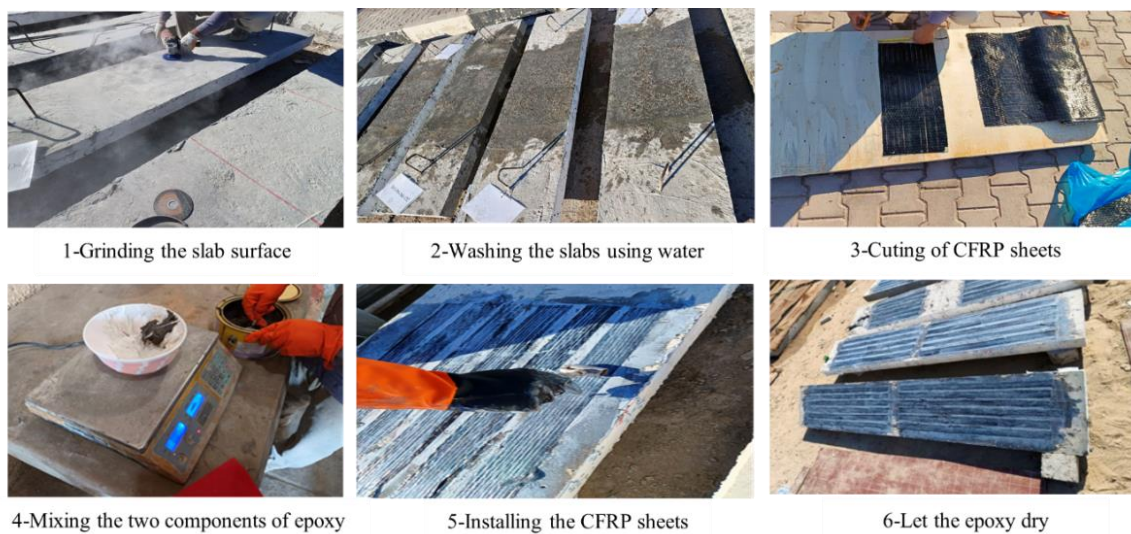


Fig. 2: Steps of repairing the RC slabs with CFRP sheets

2. Fig. 3 indicates the steps for repairing RC slabs with CFRP bars



Fig. 3. Steps of repairing the RC slabs with NSM CFRP bars.

2.2.11. Testing procedure

All Slabs were tested under a two-line load until failure. The slabs were continuous along three supports. The supports were positioned 100 mm away from the edges of the slabs resulting in clear spans of 1100 mm. Moreover, the load rate was 0.4 kN/s until the failure of the specimen, and the data of load and deflection were recorded using an LVDT. Additionally, the crack width was measured during the test. Fig. 4 illustrates the experimental test configuration while Fig. 5 displays the testing machine .

2.2.12. The configuration of EB sheets and NSM bars

The configurations of bonding EB sheets and NSM bars in positive and negative moment regions are indicated in Table 7. The CFRP sheets were glued to the center of both regions with different lengths 660 mm and 990 mm and spacing 20 mm and 40 mm. However, the spacing between the bars was 150 mm. It is worth mentioning that adopting different spacing results in a change in the number of CFRP sheets. Moreover, two of the repaired slabs were anchored to avoid debonding failure.

2.2.13. The configuration of EB sheets and NSM bars

The configurations of bonding EB sheets and NSM bars in positive and negative moment regions are indicated in Table 7. The CFRP sheets were glued to the center of both regions with different lengths 660 mm and 990 mm and spacing 20 mm and 40 mm. However, the spacing between the bars was 150 mm. It is worth mentioning that adopting different spacing results in a change in the number of CFRP sheets. Moreover, two of the repaired slabs were anchored to avoid debonding failure.

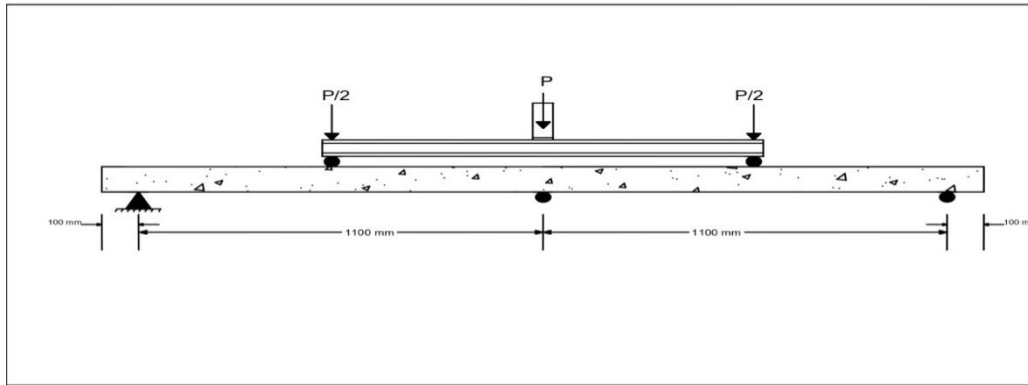


Fig. 4: Sketch for the location of supports and the applied loads



Fig. 5. Testing machine

Table 7. Configuration of EB sheets and NSM-bars on the specimens

Samples	Damage %	Sheets or bars length in positive region	Sheets or bars length in negative region	Number of sheets	End anchor
Control	-	-	-	-	-
S40-P6-N6-D2	40	0.6L	0.6L	6	Non
S40-P6-N6-D4	40	0.6L	0.6L	5	Non
S40-P9-N6-D2	40	0.9L	0.6L	6	Non
S40-P9-N6-D4	40	0.9L	0.6L	5	Non
S65-P6-N6-D2	65	0.6L	0.6L	6	Non
S65-P6-N6-D4	65	0.6L	0.6L	5	Non
S65-P9-N6-D2	65	0.9L	0.6L	6	Non
S65-P9-N6-D4	65	0.9L	0.6L	5	Non
B40-P6-N6-D15	40	0.6L	0.6L	-	Non
B65-P6-N6-D15	65	0.6L	0.6L	-	Non
AS40-P9-N6-D4	40	0.9L	0.6L	5	With
AS65-P9-N6-D4	65	0.9L	0.6L	5	With

* The meaning of the letters in the names of slabs, **S**, **B**, **AS**: Sheet, bar, and anchor sheet. **P**, **N**: Positive and negative regions. **D**: Distance. **L**: Length of one span center to center

3. RESULTS AND DISCUSSION

3.1. Ultimate load and deflection

Ultimate load and maximum deflection are presented in Table 8. It can be observed that adopting CFRPs was successful in enhancing the ultimate capacity of repaired slabs. The enhancement ratio ranges between 42% to 70%. Unfortunately, due to an accident in the laboratory during the test, the ultimate load capacity of specimen S40-P9-N6-D2 could not be determined. In the case of deflection, most of the specimens recorded a lower value of deflection than CS. The decrease in deflection ranges between 11% to 25%.

Table 8. Ultimate capacity for the continuous slabs with max deflection

Samples	Names	*Pu (kN)	Percentage of increase in ultimate load	Max deflection (mm)	Percentage of change in max deflection	Failure mode
SL1	Control	137	...	10.766	...	FF
SL2	S40-P6-N6-D2	233	70.1	8.531	-20.8	SF
SL3	S40-P6-N6-D4	221	61.3	8.084	-24.9	SF
SL4	S40-P9-N6-D2	**214	56.2	8.175	-24.1	SF
SL5	S40-P9-N6-D4	212	54.7	9	-16.4	DF
SL6	S65-P6-N6-D2	226	65.0	8.628	-19.9	DF
SL7	S65-P6-N6-D4	225	64.2	9.342	-13.2	CS
SL8	S65-P9-N6-D2	227	65.7	11.009	2.3	SF
SL9	S65-P9-N6-D4	194	41.6	9.03	-16.1	DF
SL10	B40-P6-N6-D15	198	44.5	9.573	-11.1	SF
SL11	B65-P6-N6-D15	197	43.8	7.971	-26.0	SF
SL12	AS40-P9-N6-D4	229	67.2	8.622	-19.9	CS
SL13	AS65-P9-N6-D4	212	54.7	10.786	0.2	CS

*Pu: Ultimate load, FF: Flexural failure, SF: Shear failure, DF: Debonding failure, CS: Cover separation

**This value does not represent the ultimate load for this specimen only

3.2. Ductility, stiffness and toughness

The ability of a structure to withstand inelastic deformation without experiencing a significant reduction in strength until it fails is known as ductility (Park, 1988). The stiffness (K) of an object is a measurement of the resistance to deformation provided by an elastic object (Reddy, 2003). Flexural toughness is described as the measurement of the material's capacity to absorb energy. That is the area under the load-deflection curve when stiffness is higher than or equal to zero (Hamad et al., 2019). The values of ductility, stiffness and toughness are presented in

Table 9. It can be observed that the control slab exhibits higher ductility, lower stiffness and toughness compared to the other slabs, as it does not have any strengthening at all. Moreover, when comparing the stiffness of different styles of bounding CFRP sheets, it is evident that specimen S65-P6-N6-D2 displays the highest initial stiffness, while S65-P9-N6-D2 shows the lowest value.

Table 9. Values of ductility, stiffness and toughness

Samples	Names	Ductility μ	Initial stiffness kN/mm	Toughness (kN.mm)
SL1	Control	1.73	22.4	1052.0
SL2	S40-P6-N6-D2	1.29	36.4	1253.0
SL3	S40-P6-N6-D4	1.41	39.0	1172.0
SL4	S40-P9-N6-D2	1.28	33.4	1101.0
SL5	S40-P9-N6-D4	1.39	36.2	1284
SL6	S65-P6-N6-D2	1.40	41.3	1330.0
SL7	S65-P6-N6-D4	1.38	34.2	1379.0
SL8	S65-P9-N6-D2	1.36	33.9	1731.0
SL9	S65-P9-N6-D4	1.25	35.5	1192.0
SL10	B40-P6-N6-D15	1.44	30.2	1240.0
SL11	B65-P6-N6-D15	1.56	39.2	1084.0
SL12	AS40-P9-N6-D4	1.49	40.5	1373.0
SL13	AS65-P9-N6-D4	1.56	35.3	1645.0

3.3. Crack width

To measure the crack width, a crack meter was used. When the width reached more than 0.4 mm, a crack ruler was used. The following Figures from Fig.6 to Fig. 13 illustrate the load-crack width relationships for all RC slabs. As seen in Fig.8 and Fig. 9, the positive crack of the control slab is wider than all specimens with a 65% damage ratio. However, this can't be said for all specimens with 40% damage ratio. Moreover, it can be noticed that the negative cracks are wider than positive cracks because this region has a higher moment than the positive region.

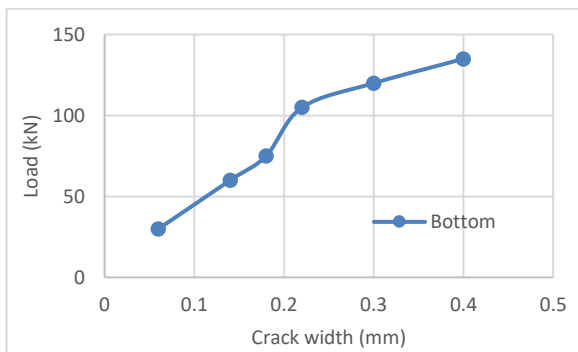


Fig.6. Crack width for positive region for control

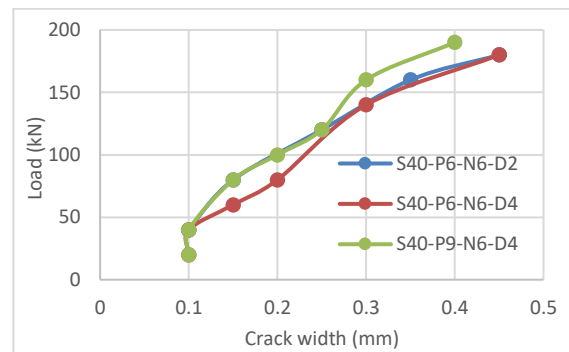


Fig.7. Crack width at negative moment region for slabs which changing their sheet length and spacing with preloading 40%

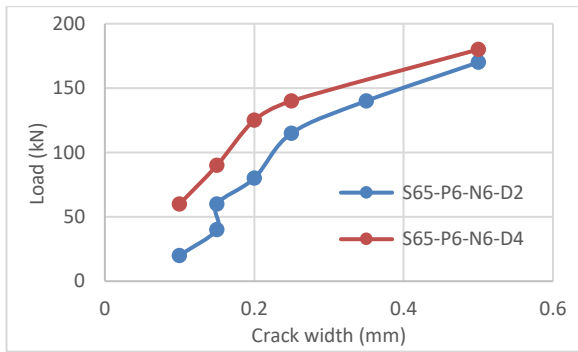


Fig. 7. Crack width at negative moment region for slabs which changing the spacing between the sheets that have 660 mm with preloading 65%

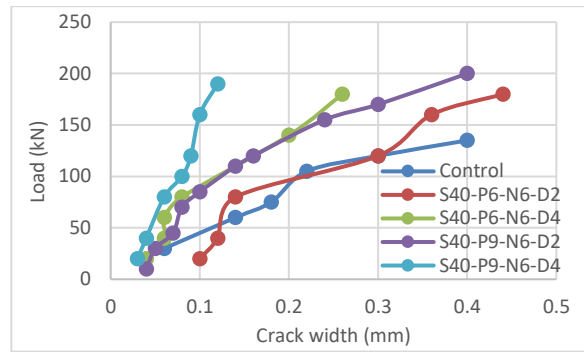


Fig.8. Crack width at positive moment region for slabs which changing their sheet length and spacing with preloading 40%

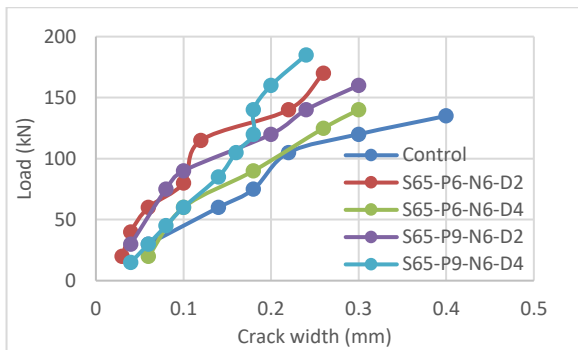


Fig. 9. Crack width at positive moment region for slabs which changing their sheet length and spacing with preloading 65%

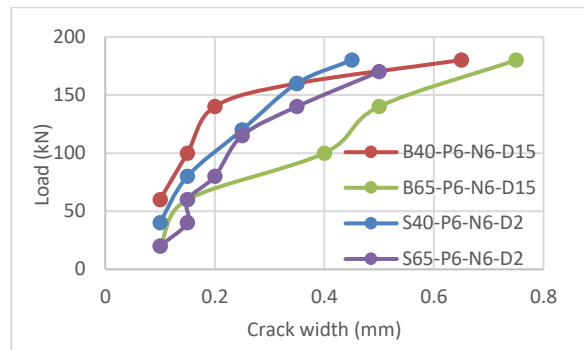


Fig. 10. Crack width at negative moment region for slabs that were strengthened with different methods (NSM and EB)

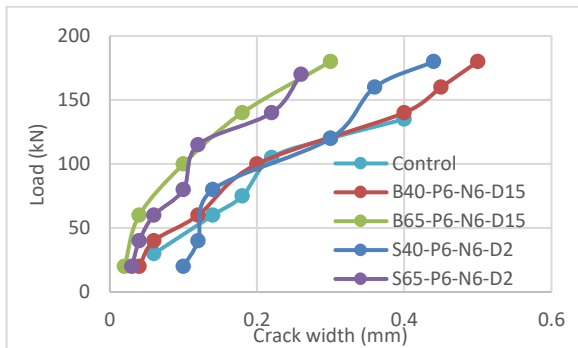


Fig.11. Crack width at positive moment region for slabs that were strengthened with different methods (NSM and EB)

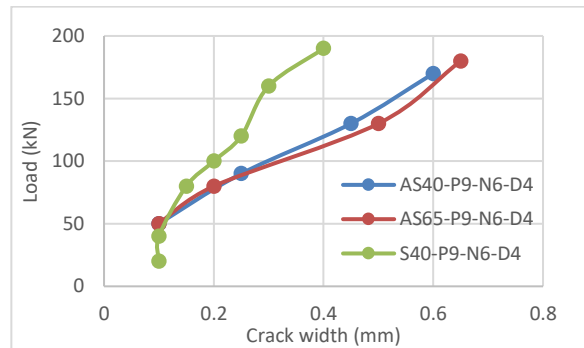


Fig. 12. Crack width at negative moment region for slabs that were anchored compared to CS and non-anchored slab

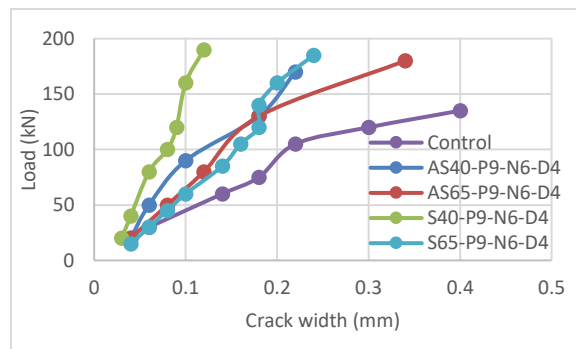


Fig. 13. Crack width at positive moment region for slabs that were anchored compared to CS and non-anchored slab

3.4. Load vs deflection curve

3.4.1. Control slab (CS)

The load-deflection curve for CS is shown in Fig.14. The failure was an ordinary flexural failure. The first loading stage, which ended with the first crack initiation at around 30 kN, shows linear behavior. In the second stage, cracks begin to appear in the concrete tension faces, but the steel bars are still within the elastic limit. This stage is usually referred to as the service stage. It can be recognized by a slight decrease in slab stiffness. The third zone is where the load value changes from 79% of its maximum capacity to the loading level at which the slab fails. This is called the ultimate load stage. A flat load-deflection curve might be obtained in this stage. The CS failed at load 137 kN according to Table 8. Moreover, it is clear from Table 9 that the control slab exhibited higher ductility, less stiffness, and less toughness than the other repaired slabs due to the absence of strengthening.

Finally, the width of the first crack of the CS with respect to the applied load is illustrated in Fig.6. A linear path can be seen in the positive moment zone. However, when the applied load exceeds 108 kN, the crack begins to expand more and more until the slab fails. This ensured that the steel would yield at this value.

3.4.2. Specimens with preloading 40%

3.4.2.1. Changing sheets length

Fig.16 represents the slabs that had a 40% damage ratio with changing their CFRP sheet length. It can be observed that the slabs with 0.9L did not achieve the highest ultimate load. This may be because when the length of the CFRP sheets is increased in the sagging region beyond the point of inflection, the extended sheets will enter the negative moment zone. Therefore, it does not effect on the compressive region of the middle span. Furthermore, it can be noticed from Table 9 that there is no effect on the ductility and no significant change in initial stiffness when increasing the length of CFRP sheets from 0.6L to 0.9L. This can be observed in Fig.16 at the early stage of loading. Additionally, all specimens that had a 40% damage ratio had higher toughness than the reference slab and S65-P9-N6-D2 had the highest value.

In the case of crack width, it can be observed from Fig. and Fig.8 that the cracks in the negative moment zone are wider than those in the positive moment zone because the negative moment is higher than the positive moment. Furthermore, convergent paths of the load-crack width can be observed in the negative cracks, because there was no change in the length of sheets in this region. While the curves in the positive cracks followed different paths. Additionally, when increasing the length of CFRP sheets the crack width reduced for all slabs.

3.4.2.2. Changing spacing between the sheets

As seen in Fig.17 and **Error! Reference source not found.**, low spacing (20 mm) between the sheets increases the ultimate load because the number of CFRP sheets is increased. However, more spacing achieved higher ductility and no change in initial stiffness according to **Table 9**. This can be noticed in load vs deflection curves in Fig.17 and **Error! Reference source not found.**. Moreover, according to **Table 9** S40-P6-N6-D2 and S40-P6-N6-D4 showed no significant change in toughness. Meanwhile, S40-P9-N6-D2 recorded lower toughness than S40-P9-N6-D4. It is important to note that S40-P9-N6-D2 failed to reach its maximum load capacity due to an accident in the laboratory. This may be the reason for these results. Furthermore, the width of the first crack decreases as the distance between the sheets increases as shown in Fig. and Fig. 7. The reason for this might be because the crack width increased as the applied load increased, at some point, the crack stopped expanding, while new cracks began to develop in other places in the concrete body.

3.4.2.3. Adopting NSM technique for repairing

To make the comparison between different strengthening methods (NSM and EB), two carbon bars with 6 mm diameter and 150 mm spacing were used in the middle of each span (positive and negative) as strengthening bars. The reason for using only two bars is to ensure that the cross-sectional area of the bar is similar to the cross-sectional area of the sheets. It can be observed from Fig.19 that there is a close path between the two slabs until 150 kN. Then, they followed different paths. S40-P6-N6-D2 shows better performance in terms of the ultimate load and reducing the deflection.

However, B40-P6-N6-D15 had a slightly more ductile behavior. This may be related to the properties of the strengthening material whereas the CFRP bars had a lower modulus of elasticity compared to CFRP sheets. This leads to wider cracks and higher deflection in the concrete, resulting in additional strain on the steel bars, causing them to yield early and exhibit more ductility. Additionally, when compared to CS, both slabs showed an improvement in the ultimate load. Moreover, according to **Table 9**, B40-P6-N6-D15 has lower stiffness than S40-P6-N6-D2 due to lower resistance to deformation. Also, there was a significant change in toughness when adopting the NSM technique. In terms of crack width, it can be noticed from Fig. 10 and Fig.11 that NSM cracks are wider than EB due to the same reason mentioned earlier and tend to take separate paths in the negative region. However, the curves of load vs crack width are a little convergent in the positive region.

3.4.2.4. Adopting end-anchors

Both S40-P9-N6-D4 and AS40-P9-N6-D4 in Fig.20 had a 40% damage ratio and were strengthened with the same configuration of CFRP sheets, except that AS40-P9-N6-D4 was anchored at the ends of each strengthening sheet to prevent debonding failure. It can be noticed that the slope of the curve (stiffness) starts to decrease at about 190 kN progressively due to the appearance of additional cracks in the concrete. Additionally, the primary finding was that the ultimate load capacity of the S40-P9-N6-D4 specimen increased by about 7% whereas the deflection was reduced by a little bit when adopting end anchors. Moreover, adopting end-anchors results in increasing the ductility, initial stiffness, and toughness by 7.19 %, 11.87%, and 6.93% according to

Table 9.

Finally, AS40-P9-N6-D4 has a wider crack than S40-P9-N6-D4 according. Finally, AS40-P9-N6-D4 has a wider crack than S40-P9-N6-D4 according to Figs.13 and 14 due to the development of an additional crack in the specimen.

3.4.3. Specimens with preloading 65%

3.4.3.1. Changing sheet lengths

As seen in Fig.21, S65-P6-N6-D2 and S65-P9-N6-D2 had the greatest ultimate capacity among the others, while S65-P9-N6-D4 had the lowest value. Also, it can be noticed that all slabs had convergent paths except S65-P6-N6-D2 which shows higher stiffens than the others. Moreover, it is easy to note that using longer sheets did not lead to any enhancement in the ultimate load capacity.

As seen in Table 9, the specimens S65-P6-N6-D2 and S65-P6-N6-D4 have higher ductility than S65-P9-N6-D2 and S65-P9-N6-D4 respectively. This may be due to the tension region will be covered by more sheets. In terms of initial stiffness, changing sheet lengths does not affect stiffness. Additionally, from Table 9, all slabs with a 65 % damage ratio show greater toughness than CS due to the presence of strengthening. The percentage of increase in toughness ranges between 3% and 65%

Lastly, it can be seen in Fig. 9 that the repairing techniques tend to reduce crack width. Also, S65-P6-N6-D2 recorded a lower crack width than S65-P9-N6-D2 in the positive region due to the appearance of additional cracks in the concrete body. However, S65-P6-N6-D4 recorded a wider crack than S65-P9-N6-D2. This may be because S65-P6-N6-D4 has a higher ultimate load than S65-P9-N6-D2 resulting in wider crack width.

3.4.3.2. Changing spacing between the sheets

Increasing the spacing between the sheets will decrease their number and consequently reduce the ultimate load. This can be seen in Fig. and Fig.15. Additionally, no change in ductility between S65-P6-N6-D2 and S65-P6-N6-D4 has been seen. But, S65-P9-N6-D2 shows higher ductility than S65-P9-N6-D4 by about 8.8%. Moreover, when the spacing was increased from 20 mm to 40 mm for specimen S65-P6-N6-D2, it was recorded less stiffness. However, there was no change in initial stiffness between S65-P9-N6-D2 and S65-P9-N6-D4 according to Table 9. In terms of toughness, S65-P9-N6-D2 recorded the highest value and it's significantly higher than S65-P9-N6-D4 by about 45%. However, there was no effect of spacing on toughness when compared between S65-P6-N6-D2 and S65-P6-N6-D4. According to Fig. 7 and Fig. 9, there was no significant change in crack width in the negative region. In the positive region S65-P6-N6-D2 specimen that has less spacing exhibits a smaller crack width compared to S65-P6-N6-D4. However, S65-P9-N6-D2 shows a higher crack width than S65-P9-N6-D4.

3.4.3.3. Adopting NSM technique for repairing

S65-P6-N6-D2 was strengthened with EB-CFRP sheets while B65-P6-N6-D15 was strengthened with NSM carbon bars. As seen in Fig.24, all the curves of the slabs have similar paths until the appearance of the first crack. After that, they took separate paths and recorded a decrease in deflection. Additionally, both techniques enhanced the ultimate load capacity by 65% for EB and 43.8% for NSM compared to CS. It can be observed that adopting the NSM method shows higher ductility than CFRP sheets by 11.43%, no change in initial stiffness, and less toughness by about 18.5% according to Table 9. In terms of crack width, the specimens that were strengthened with NSM carbon bars show a higher value of crack width compared to CFRP sheets in both regions as indicated in Fig. 10 and Fig.12.

3.4.3.4. Adopting end-anchors

The strengthening sheets were anchored at their ends by one layer of CFRP sheet with dimensions of (50 mm) in width and (700 mm) in length. For AS65-P9-N6-D4, end anchors were used on the top and bottom sides. When comparing S65-P9-N6-D4 and AS65-P9-N6-D4 in Fig. 25, it can be noticed that adding anchors to the slabs leads to an increase in the ultimate load capacity by about 9.27%. This may happen because of inducing the internal tensile force (catenary action) in CFRP sheets which means at a high stage of loading, the member stiffness may be increased or in other words when the deflection value becomes high. When cracks start to form and steel reinforcement begins to yield, additional cracks develop in the tension zone, relieving the concrete of stresses, and causing the sheet fibers to carry larger loads than the concrete. Adopting end-anchors in repairing slabs results in increase in the ductility by about

24.8% compared to a non-anchored slab, with no change in initial stiffness and increased toughness according to Table 9. Additionally, wider cracks can be noticed in Figs. 13 and 14 for AS65-P9-N6-D4 compared to S65-P9-N6-D4.

3.4.4. Damage ratio

Two damage ratios were applied to the RC slabs: 40% and 65%. According to ductility

Table 9, the majority of slabs with a 40% preloading ratio recorded lower values of ductility compared to slabs with a 65% preloaded ratio. This may be because, at a 65% damage ratio, the number of cracks is higher. Additionally, most of the loads were carried by strengthening materials and reinforcement steel. This may be due to the strain for all materials (concrete with sheet or bar) being equal but the stress that is transported to the concrete is less than the repairing materials. Furthermore, it can be observed that there was a slight change in the initial stiffness for most non-anchored slabs when increasing the damage ratio from 40% to 65%. However, for the anchored slab (AS65-P9-N6-D4), the initial stiffness decreased by 12.83% compared to (AS40-P9-N6-D4). Also, in NSM specimens the stiffness increased by 29.8% when adopting a higher damage ratio. In the case of toughness, most of the specimens that had a 65% damage ratio showed higher toughness than those with a 40% damage ratio. For example, S65-P6-N6-D2 recorded a higher value than S40-P6-N6-D2 by about 6.15%.

Finally, it was observed from Fig.7 to Fig. 13 of load vs crack width curves that specimens with a 65% damage ratio have wider negative cracks than those with a 40% damage ratio due to the high damage ratio creating more and wider cracks in the slab. This can be said for the positive cracks except for the NSM specimen (AS65-P6-N6-D15).

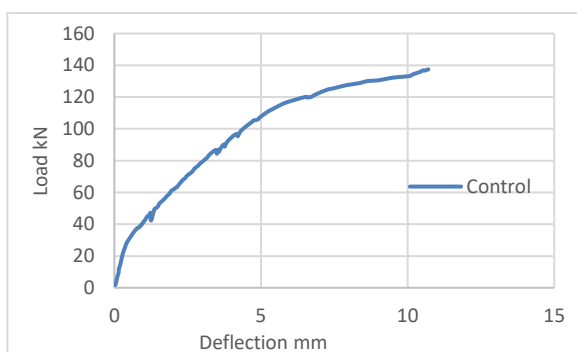


Fig.14. Load-deflection curve of CS specimen

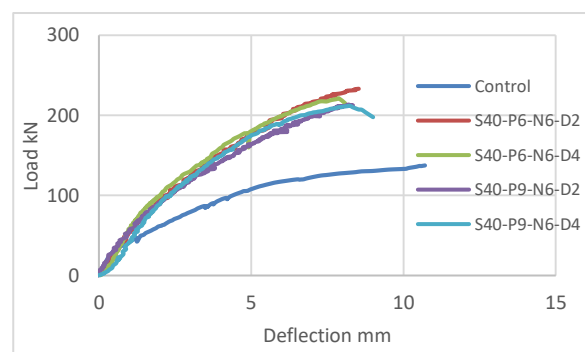


Fig.16. Load vs deflection curves for slabs which changing their sheet lengths with preloading 40%

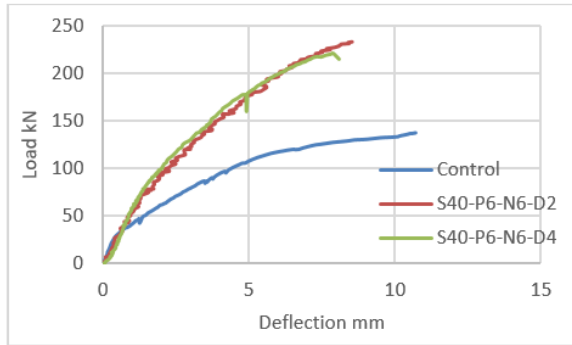


Fig.17. Load vs deflection curves for slabs which have 660 mm CFRP sheet length and different spacing with 40 % preloading ratio

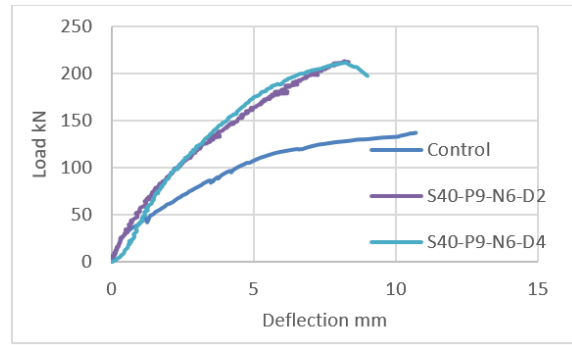


Fig.18. Load vs deflection curves for slabs which have 990 mm CFRP sheet length and different spacing with 40 % preloading ratio

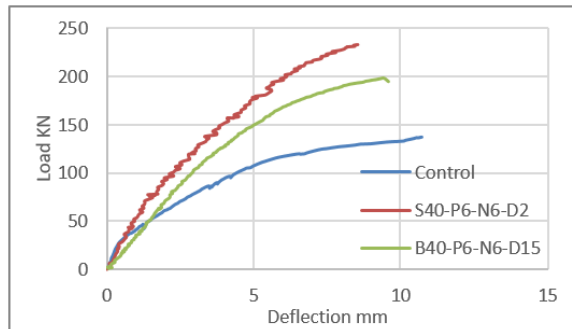


Fig.19. Load vs deflection curves for slabs that were repaired with different techniques and preloading 40%

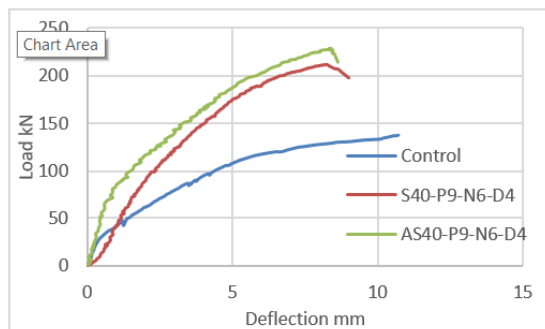


Fig.20. Load vs deflection curves for slab that were anchored compared to CS and non-anchored slab for a 40% preloading

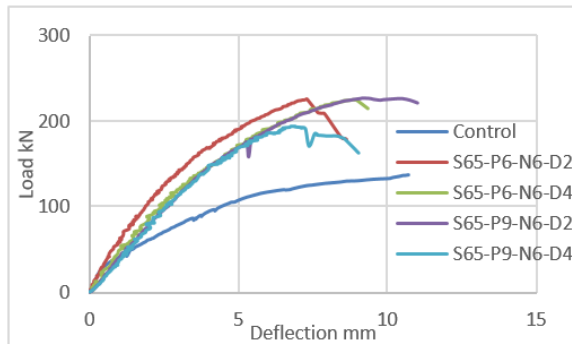


Fig.21. Load vs deflection curves for slabs which changing their sheet lengths with preloading 65%

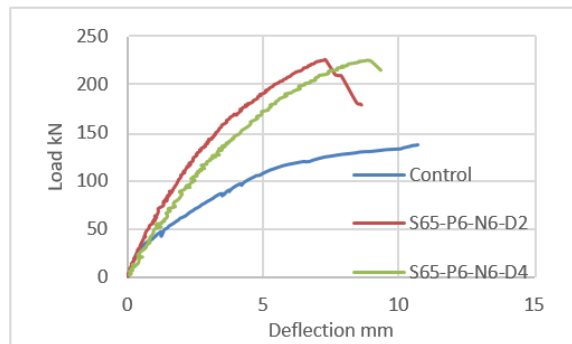


Fig.22. Load vs deflection curves for slabs which have 660 mm CFRP sheet length and different spacing with 65 % preloading ratio

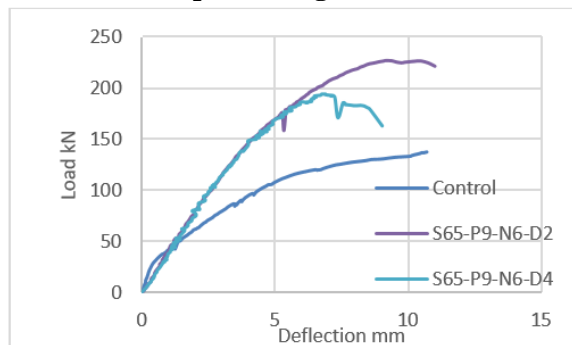


Fig.15. Load vs deflection curves for slabs which have 990 mm CFRP sheet length and different spacing with 65 % preloading ratio

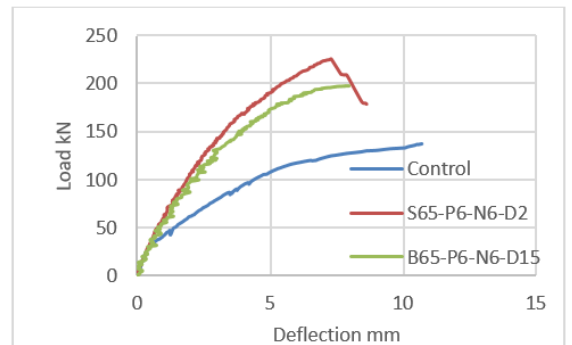


Fig.24. Load vs deflection curves for slabs that were repaired with different techniques and preloading 65%

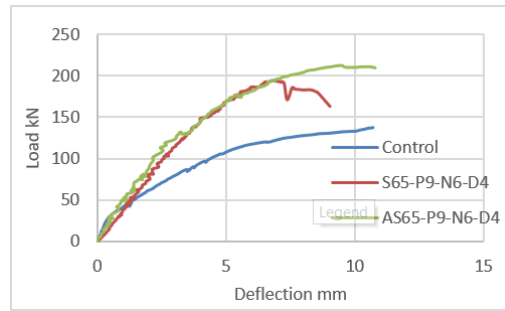


Fig.25. Load vs deflection curves for slab that were anchored compared to CS and non-anchored slab for a 65% preloading

4. CONCLUSIONS

1. The following points will provide an overview of the primary conclusions that were made. EB technique is considered a simple and effective method for repairing damaged concrete slabs.
2. Both EB and NSM enhanced the ultimate load capacity compared to the control slab by about. However, the EB shows better performance in terms of improving the ultimate load and reducing the deflection.
3. Increasing the length of CFRP sheets didn't lead to any improvement in ultimate load compared to similar slabs that had less sheet length. Moreover, there was no effect on ductility and stiffness at 40% preloaded ratio but at 65% the effect of length was clear in reducing the ductility by about 2.85% and 9.42%.
4. Increasing the number of CFRP sheets by reducing the spacing between them lead higher ultimate load, less ductility and no change in initial stiffness.
5. Adopting NSM method results in increasing the ductility by 11.63%, reducing the stiffness by 17% and no change in toughness for 40% preloaded ratio. However, for 65% higher ductility by 11.43%, no change in stiffness and less toughness by about 18.5%.
6. Adopting end-anchors was effective in avoiding debonding failure.
7. The effect of CFRP sheet performance in inducing the catenary action was notable in the 65% preloaded ratio.
8. When the damage ratio is decreased to 40%, the majority of slabs recorded reduce in ductility by about 8.52%, 6.25%, 8.33%, and 4.7% for S40-P6-N6-D2, S40-P9-N6-D2, B40-P6-N6-D15 and AS40-P9-N6-D4 respectively. Furthermore, most of the specimens that had a 65% damage ratio show higher toughness and wider negative cracks than those with a 40% damage.

5. REFERENCES

Aram, M.R., Czaderski, C. and Motavalli, M. (2008) "Debonding failure modes of flexural FRP-strengthened RC beams. Composites part B", engineering, 39(5), 826-841.

ASTM A615/615M-05a (2005) “Standard Specification for Deformed and Plain Carbon Structural Steel Bars for Concrete Reinforcement”, Annual Book of ASTM Standards, Vol.01.02.

ASTM C494/C494M-15 (2015) “Standard Specifications for Chemical Admixtures for Concrete”, Developed by ASTM Subcommittee C09.23, Vol. 04.02, West Conshohocken, PA, USA.

ASTM C496/C496M (2011) “Standard Test Method for Splitting Tensile Strength of Cylindrical Concrete Specimens” USA: ASTM International, 1-5.

ASTM C78/C78M (2015) “Standard Test Method for Flexural Strength of Concrete (Using Simple Beam with Third-Point Loading)” USA: ASTM International, 1-4.

B. S. Institution, Specification for Testing Concrete: Method for Determination of the Compressive Strength of Concrete Cores. British Standards Institution, 1983.

Benjeddou, O., Ouezdou, M.B. and Bedday, A. (2007) “Damaged RC beams repaired by bonding of CFRP laminates”, Construction and building materials, 21(6), 1301-1310.

De Lorenzis, L. and Teng, J.G. (2007) “Near-surface mounted FRP reinforcement: An emerging technique for strengthening structures. Composites Part B”, Engineering, 38(2), 119-143.

Fayyadh, M.M. and Razak, H.A. (2012) “Assessment of effectiveness of CFRP repaired RC beams under different damage levels based on flexural stiffness. Construction and Building”, Materials, 37, 125-134.

Frhaan, W.K.M., Abu Bakar, B.H., Hilal, N. and Al-Hadithi, A.I. (2021) “CFRP for strengthening and repairing reinforced concrete: A review”, Innovative Infrastructure Solutions, 6, 1-13.

Hamad, A.J. and Sldozian, R.J.A. (2019) “Flexural and flexural toughness of fiber reinforced concrete-American standard specifications review”, GRD Journals-Global Research and Development Journal for Engineering, 4(3), 5-13.

Hosen, M.A., Jumaat, M.Z., Darain, K.M.U., Obaydullah, M. and Islam, A.S. (2014) “Flexural strengthening of RC beams with NSM steel bars. In Proceedings of the International Conference on Food”, Agriculture and Biology (FAB-2014), Kuala Lumpur, Malaysia.

https://gcc.sika.com/content/dam/dms/gcc/8/sikawrap_-300_c.pdf

<https://irq.sika.com/content/dam/dms/iq01/h/sikadur-330.pdf>

<https://www.anjiezj.com/carbon-fiber-rebar>

https://www.middleeast.weber/files/sodamco/2018-05/weberep_epo_412_CRY_01.pdf

Iraqi Specification No. 45 (1984) “Natural Sources for Gravel that is used in concrete and construction”, Baghdad.

Iraqi Specification No. 5, (1984) “Portland Cement”, Baghdad.

Kamonna, H.H. and Abd Al-Sada, D.J. (2021) “Strengthening of one-way reinforced concrete slabs using near surface mounted bars. *Materials Today*”, Proceedings, 42, 1843-1853.

Li, G., Zhang, A. and Jin, W. (2014) “Effect of shear resistance on flexural debonding load-carrying capacity of RC beams strengthened with externally bonded FRP composites”, *Polymers*, 6(5), 1366-1380.

Martinelli, E., Napoli, A., Nunziata, B. and Realfonzo, R. (2014) “RC beams strengthened with mechanically fastened composites: Experimental results and numerical modeling”, *Polymers*, 6(3), 613-633.

Matthys, S. and Taerwe, L. (2000) “Concrete slabs reinforced with FRP grids. II: Punching resistance”, *Journal of Composites for Construction*, 4(3), 154-161.

Park, R. (1988) Ductility evaluation from laboratory and analytical testing. In Proceedings of the 9th world conference on earthquake engineering 8, 605-616). Tokyo-Kyoto Japan.

Reddy, J. N. (2003) *Mechanics of laminated composite plates and shells: theory and analysis*. CRC press.

Teng, J.G., Chen, J.F., Smith, S.T. and Lam, L. (2003) “Behavior and strength of FRP-strengthened RC structures: a state-of-the-art review”, *Proceedings of the institution of civil engineers-structures and buildings*, 156(1), 51-62.

Thi, C.N., Pansuk, W., and Torres, L. (2015) “Flexural behavior of fire-damaged reinforced concrete slabs repaired with near-surface mounted (NSM) carbon fiber reinforced polymer (CFRP) rods”, *Journal of Advanced Concrete Technology*, 13(1), 15-29.

Wong, R.S.Y. (2001) *Towards modelling of reinforced concrete members with externally-bonded fiber reinforced polymer, FRP, composites* (Doctoral dissertation).